Ternary Vapor–Liquid Equilibrium Measurements and Modeling of Ethylene Glycol (1) + Water (2) + Methane (3) Systems at 6 and 12.5 MPa

Kruger, Francois J.; Danielsen, Marie V.; Kontogeorgis, Georgios M.; Solbraa, Even; von Solms, Nicolas

Published in:
Journal of Chemical and Engineering Data

Link to article, DOI:
10.1021/acs.jced.8b00115

Publication date:
2018

Document Version
Peer reviewed version

Ternary vapor-liquid equilibrium measurements and modeling of ethylene glycol (1) + water (2) + methane (3) systems at 6 and 12.5 MPa

Francois J. Kruger[‡], Marie V. Danielsen[†], Georgios M. Kontogeorgis[‡], Even Solbraa[†], Nicolas von Solms[‡,]*

‡ Department of Chemical and Biochemical Engineering, Center for Energy Resources Engineering (CERE), Technical University of Denmark, DK-2800, Lyngby, Denmark

† Statoil ASA, Research and Development Center, N-7005, Trondheim, Norway

ABSTRACT

Novel technologies in the field of subsea gas processing include the development of natural gas dehydration facilities, which may operate at high pressure due to their proximity to reservoirs. For the qualification and design of these processing units, ternary vapor-liquid equilibrium data are required to validate the thermodynamic models used in the design process. For this purpose, 16 new ternary data points have been measured for ethylene glycol (1) + water (2) + methane (3) at 6.0 and 12.5 MPa, with temperatures ranging from 288 to 323 K and glycol content above 90 wt%. Glycol in gas (y_1), water in gas (y_2) and methane solubility (x_3) have been measured with relative experimental uncertainties ($u_r(x) = u(x) / |x|$) below 12 %, depending on the type of data. The Cubic-Plus-Association (CPA) equation of state has been used to model the data. Literature pure component and binary interaction parameters have been used. It is found that the model provides a good qualitative description of the experimental data for y_1 and y_2, while a significant over prediction occurs for x_3. The modeling errors for CPA ranged between 5 – 40 % average absolute relative deviation.

INTRODUCTION

Mono-ethylene glycol (MEG) (IUPAC: 1,2-ethanediol) is used in oil & gas industry as both a hydrate inhibitor in gas transport lines and dehydrating agent for gas processing applications. The use of MEG has been considered for high-pressure subsea natural gas dehydration[1] and process designs for such applications require phase equilibria measurements for gas-water-glycol mixtures. This is crucial for the design the separation equipment, where the critical product specifications are the water and glycol content of the vapor phase. Sales Gas specifications vary from region to region, but are generally in line with those specified by GASSCO:[2]

- Water dew point -18 °C at 6.9 MPag
- Max. daily average glycol content 8 $L \cdot MSm^{-3}$

These stringent specifications are in place to prevent corrosion and ensure asset integrity in downstream transport networks, but present a significant challenge in terms of process design. Tri-ethylene glycol (TEG) is typically preferred for industrial dehydration applications as it can reach a lower water dew point and is less volatile. This results in lower glycol carry-over into the product stream. MEG, however, offers dual purpose capability (inhibition & dehydration) and improved economics. Additionally, its lower viscosity aids direct injection applications, especially at lower temperatures.[3]

Very few glycol-related data sets are found in the open literature. Natural gas related binary data for MEG consists mainly of gas solubility measurements[4–11] in mixtures with methane, ethane, nitrogen and carbon dioxide. Most literature sources for modeling applications advocate the use of data from the research groups of Jou[4,7] or Zheng[5]. Due to the difficulties in quantifying vapor-

phase glycol content, only a few sources[8,12] present this type of data. Furthermore, only two sources[6,8] provide ternary gas-water-glycol data and only Folas *et al*.[8] present data for both phases. A few more data sets appear in sources not within the open literature, such as the Gas Processors Association (GPA). Data for $CH_4 + C_3H_8 + MEG + H_2O$ and $CH_4 + CO_2 + MEG + H_2O$ measured by Ng & Chen[13] is shown in Boesen *et al*.[14]

Given this relative dearth of available data, we aim to generate new experimental data for ternary systems ($MEG + H_2O + CH_4$) relevant to subsea natural gas dehydration applications. The experimental conditions are varied with temperature, pressure and glycol composition within the following ranges: T = (288 – 323) K, p = (6.0 – 12.5) MPa and *MEG content* = (90 – 99) wt%.

Although the main aim of this work is to generate experimental data, the ability of thermodynamic models to describe this data accurately is also essential for the process design of natural gas dehydration and related processes. Several models could be of interest here. An upgraded version of the Soave-Redlich-Kwong (SRK)[15] equation incorporates an excess Gibbs energy mixing rule developed by Huron & Vidal[16], often referred to as SRK-HV. Several relevant systems have been modelled using SRK-HV[8,14,17] and it has been incorporated in several modelling packages e.g. Aspen Plus and PVTsim. Similarly, CPA[18,19] is of specific interest to natural gas dehydration applications as it is purpose-built for considering the interaction between hydrocarbons and associating compounds e.g. water and glycol. Liang *et al*.[20] provide a systematic and extensive comparison of CPA with sPC-SAFT for several systems of interest to this work, while other authors have considered the application of CPA for hydrate inhibition studies.[21–23] Folas *et al*.[8] achieved a fair description of their $MEG + H_2O + CH_4$ data using CPA. CPA has also been incorporated in industrial process design software, where natural gas dehydration units were modelled.[24] Natural gas hydrate formation has also recently been modelled with the using of

machine-learning techniques[25,26] where the best results were achieved using three-layer artificial neural networks.

Given that association interactions are specifically accounted for and the relative simplicity of CPA, it has been chosen for comparison with the experimental data generated in this work.

EXPERIMENTAL SECTION

APPARATUS

The experiments were conducted using the experimental apparatus and analytical techniques of Folas *et al*.[8]. Due to difficulties with the hydraulic and cooling systems, the cell body and refrigeration unit were replaced. The analytical equipment and techniques have remained unchanged, apart from the incorporation of the improved GC-MS method of Miguens *et al*.[12] for the analysis of MEG in the vapor phase. Vapor-liquid equilibrium is established inside a 450 mL nickel-alloy cell. The cell is located inside a climate chamber which has a range of T = (223.15 – 473.15) K with temperature control to within ± 0.05 K. The pressure and volume can be manipulated by hydraulic pistons and a magnetic stirrer ensures sufficient contact between the phases. The apparatus was designed and built by Sanchez Technologies (now Core Laboratories) and is shown in Figure 1. The climate chamber, equilibrium cell and control systems appear on the right side.

The vapor-liquid interface can be observed through a sight glass and the apparatus is equipped with a camera for remote visual observation. The pressure inside the cell is measured using a Keller Pax 33X digital pressure transmitter [range: p = (0.000 to 100.000) MPa (abs), accuracy: < 0.2%]. The temperature of the cell wall is measured using a PT100 element and P655-Ex digital thermometer (Dostman Electronic) with a stated accuracy of ± 0.05 K.

The cell may be loaded with gas or evacuated via V-2A/B, while the contents of the cell may be accessed through two pathways (V-1A/B and V-3A/B) (see the left side of Figure 1). The cell is filled with liquid via V-3A/B.

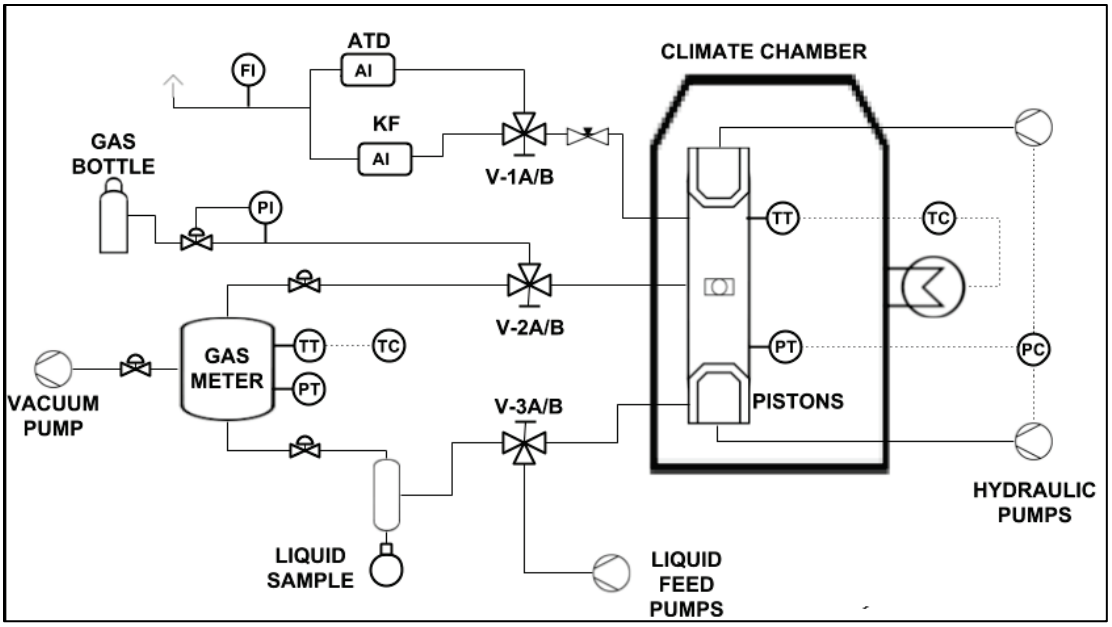

Figure 1 Experimental apparatus for high-pressure vapor-liquid equilibrium measurements of systems containing glycol, water and natural gas.

Sampling is achieved through one of three pathways. Vapor can be routed via valves V-1A/B for Karl Fischer (KF) analysis or adsorption in stainless steel automated thermal desorption (ATD) tubes (Tenax® TA from Perkin Elmer). The vapor flow rate is measured (see FI in Figure 1) using a drum-type gas meter (Ritter TG 1/5) calibrated for a volumetric flow of $\dot{V}$ = (2 – 120) $L \cdot h^{-1}$ (deviation: 0.09% @ 100 $L \cdot h^{-1}$). Liquid samples are flashed to a gas-liquid separator, via valve V-3A. The *'flash gas'* is collected in a temperature-controlled variable-volume gas meter. The pressure inside the gas meter is measured using a Keller Pax 33X digital pressure transmitter which has a range of p = (0.000 to 1.000) MPa (abs) with an accuracy better than 0.01% of full scale given on the calibration certificate. The pressure in the gas meter is controlled through the motion of a hydraulic piston, with the volume measured to within ± 0.01 mL.

MATERIALS

Three compounds were used in this work and no additional purification was performed. The specifications provided by the suppliers are shown in Table 1.

Table 1 List of materials used in this work

No.	Name	CAS No.	Supplier	Purity	Water content	Additional purification
1	MEG	107-21-1	Sigma-Aldrich (324558)	99.8 mol%	< 0.003 % (by KF)	None
2	H_2O	7732-18-5	ELIX® Reference 5	Resistivity @ 298.15 K: 10-15 μS/cm	N/A	None
3	CH_4	74-82-8	Air Liquide (N55)	99.9995%	< 2 ppm	None

EXPERIMENTAL PROCEDURE

The equilibrium cell is first washed with acetone and then placed under vacuum for 2-3 hours with $p < 0.20$ kPa. Depending on the desired experimental pressure (6.0 or 12.5 MPa), either 260 or 200 ± 5 mL of methane is loaded from the gas bottle via valve V-2B. 60 ± 2 mL of a prepared liquid mixture is pumped into the cell. The molar feed ratios range from $z_1 = (0.41 – 0.65)$, $z_2 = (0.02 – 0.18)$ and $z_3 = (0.31 – 0.48)$ for the various experiments. Further details about the experimental conditions are given in Table 2. These feed compositions are significantly different from those of Folas *et al.*[8] who used a feed ratio of $z = (0.1855, 0.622, 0.1925)$.

Table 2 Experimental conditions at Temperature T, Pressure p and Component Molar Feed Fraction z_i for the study of ternary system: ethylene glycol (1) + water (2) + methane (3)

Exp. No.	T/K	p/MPa	z_1	z_2	z_3
1	288.20	5.93	0.498	0.171	0.331
2	293.13	6.00	0.499	0.172	0.330
3	298.29	5.99	0.502	0.173	0.325
4	303.14	6.00	0.504	0.173	0.322
5	313.15	6.01	0.509	0.175	0.316
6	323.16	5.99	0.515	0.177	0.308
7	288.16	12.53	0.413	0.142	0.446
8	293.14	12.47	0.417	0.143	0.440
9	298.29	12.47	0.420	0.144	0.436
10	303.14	12.50	0.422	0.145	0.432
11	313.15	12.49	0.428	0.147	0.424
12	323.19	12.50	0.434	0.149	0.417
13	298.23	5.99	0.563	0.092	0.346
14	298.23	12.47	0.466	0.076	0.458
15	298.18	5.98	0.617	0.019	0.363
16	298.17	12.47	0.506	0.016	0.478

Once the cell is loaded, the stirrer is turned on and the process is left to equilibrate for a minimum of 16 hours. Pressure, temperature and volume are recorded. Gas dissolves into the liquid phase until a constant PVT condition (within the range: $p \pm 1$ kPa, $T \pm 0.01$ K and $V \pm 0.01$ mL) is reached, typically within the first 6 hours.

SAMPLING AND ANALYSIS

Once equilibrium is achieved, sampling can commence. The entire sampling pathway, including the gas meter, is evacuated before the liquid sample is taken. The sample space is then pressurized to 115 kPa with helium to minimize atmospheric ingress. The tubing between the cell and the separator is flushed with approximately 5 mL of liquid from the cell before a single 25 mL sample is taken via valve V-3B. The effect of the sample volume on the equilibrium was considered using the CPA equation of state. The maximum expected disturbance was estimated as ≤ 0.1 % of the experimentally measured results. During liquid sampling the lower hydraulic piston is activated to maintain the equilibrium pressure in the cell. Manipulation of the sampling valve introduces pressure variation, with $p = \pm 50$ kPa deemed acceptable, while variations of less than ± 20 kPa were typically observed.

Depressurization of the liquid during sampling causes dissolved methane to flash into the gas meter. While a small portion of the liquid components would also vaporize into the flash gas, it was estimated that the flash gas would consist of ≥ 99.7% methane. The change in volume of the gas meter (under constant pressure and temperature) is recorded, giving the volume of *'flash gas'*. Additionally, the liquid sample mass (Ohaus Explorer Pro, $m \pm 0.001$ g), water content (Metrohm 915 KF Ti-Touch, $u(x_{H2O}) = \pm 2\%$) and density (Anton Paar DMA 4500M, $\rho \pm 0.00007$ g mol^{-1}) are measured. These measurements are used to determine the dissolved methane content, with the relevant calculations demonstrated in equations S1 – S4 (see Supporting Information).

Water content of the gas phase is measured by routing vapor via valve V-1B to a coulometric KF analyzer (Metrohm 831 KF Coulometer, $u(y_{H2O}) = \pm 3\%$). Depending on the volume of gas available and the stability of the measurement, between 5 and 15 parallel samples were taken.

Gas samples (typically 10 samples of 0.5 L each) are routed through ATD tubes via valve V-1A. MEG adsorbs onto the Tenax® coating of the ATD tubes and is then later thermally desorbed for analysis. Analysis is done using an Agilent 5975C GC-MS, which is fitted with a Varian CP7448 (*length* = 60 m, *diameter* = 320 μm) capillary column. Duplicate three-point calibration (versus standard solutions) was performed for each batch of samples. The resultant MEG mass, and sample volume, is used to calculate MEG vapor composition (y_1) using equations S5 – S7 (see Supporting Information).

EXPERIMENTAL UNCERTAINTY

The values for w_2 (KF Volumetric), y_1 (KF Coulometric) and y_2 (GC-MS) are reported as the mean of all the parallel measurements, while x_3 is calculated using the mean values (where appropriate) of the measured quantities. For directly measured results (KF and GC-MS), the experimental uncertainty is reported as three standard deviations of the parallel measurements in Table S1 (see Supporting Information). Experimental uncertainties for the methane solubility (x_3) are determined through Monte Carlo simulations using equations S1 – S4 (see Supporting Information) and the standard deviations for the various measurements incorporated in the calculation. Where only a single measurement is taken (e.g. T and p), the instrument uncertainty is used in the calculation. Unless stated otherwise, we present uncertainty in the relative form i.e. $u_r(x) = u(x) / |x|$.

THERMODYNAMIC MODELING

The Cubic-Plus-Association[18] (CPA) equation of state (EoS) was developed to combine the simplicity of traditional cubic equations of state (specifically the Soave-Redlich-Kwong[15] (SRK) EoS) with the association term of the Statistical Association Fluid Theory (SAFT). In this work we have used the 1999 version of CPA[19] which incorporates a simplified radial distribution function (*g*). The full set of equations are given by Kontogeorgis and Folas[27], with a summarized version shown here in equations 1-5.

$$p = p_{SRK} + p_{assoc}$$
$$= \frac{RT}{V_m - b} - \frac{a(T)}{V_m(V_m + b)} - \frac{RT}{2V_m}\left(1 + \rho_m \frac{\partial \ln g}{\partial \rho_m}\right)\sum_i x_i \sum_{A_i}\left(1 - X_{A_i}\right)$$

Eq. 1

The first two terms in Eq. 1 relate to the classical SRK repulsive and attractive components, where *b* refers to the molecular co-volume, V_m is the molar volume and *a(T)* refers to the temperature-dependent attractive interaction. *a(T)* is described in terms of the attractive energy (a_0) and dimensionless temperature-correction (c_1) shown in Eq. 2.

$$a(T) = a_0\left(1 + c_1\left(1 - \sqrt{T_R}\right)\right)^2$$

Eq. 2

In CPA, the energy parameter is often shown in reduced form: $\Gamma = a_0/(b \cdot R)$ where R is the universal gas constant. The third term in Eq. 1 describes the association interaction in terms of the molar density ($\rho = 1/V_m$), the mole fraction of nonbonded sites (X_{Ai} see Eq. 3) for association site A on molecule i, association strength (Δ^{AiBj} see Eq. 4) and radial distribution function ($g(\rho)$ see Eq. 5).

$$X_{A_i} = \frac{1}{1 + \rho \sum_j x_j \sum_{B_j} \left(X_{B_j} \Delta^{A_i B_j} \right)}$$

Eq. 3

$$\Delta^{A_i B_j} = g(\rho) \left[\exp\left(\frac{\varepsilon^{A_i B_j}}{RT} \right) - 1 \right] b_{ij} \beta^{A_i B_j}$$

Eq. 4

$$g(\rho) = \frac{1}{1 - 1.9\eta} \; where \; \eta = \frac{1}{4b\rho}$$

Eq. 5

Δ^{AiBj} is defined by the association interaction between site A on molecule i and site B on molecule j and requires the definition of an additional two pure component parameters: the association energy (ε) and volume (β).

Literature parameters for MEG, water and methane (shown in Table 3) were used in this work.

Table 3 CPA parameters for modeling of ethylene glycol, water and methane

	b / $cm^3 \cdot mol^{-1}$	Γ / K	c_1	ε/R / K	$\beta \cdot 10^3$	Association Scheme	Ref.
MEG	51.4	2531.71	0.6744	2375.752	14.1	4C	Derawi *et al.*[28]
H_2O	14.515	1018.39	0.67359	2003.25	69.2	4C	Kontogeorgis *et al.*[19]
CH_4	29.1	959.028	0.44718	-	-	-	Tsivintzelis et al.[29]

Conventional mixing rules for the a and b parameters are given by:

$$a(T) = \sum_i \sum_j x_i x_j a_{ij}(T) \;\; with \;\; a_{ij}(T) = \sqrt{a_i(T) \cdot a_j(T)} \left(1 - k_{ij}\right)$$

Eq. 6

$$b = \sum_i x_i b_i$$

Eq. 7

where k_{ij} is the binary interaction parameter (BIP).

CPA has been shown to be predictive for mixtures of natural gas and water, giving comparable performance to the empirical GERG-water correlation[30], but with the incorporation of MEG, single BIPs were required.

For comparative purposes, we have used the same BIPs as Folas *et al.*[8] for the modeling of the data:

- k_{12} = -0.115 (MEG – H_2O)
- k_{13} = 0.134 (MEG – CH_4)
- k_{23} = -0.045 (H_2O – CH_4)

Elliot's combining rule (ECR) has been recommended the cross-association interactions between MEG and water[8,27,31], and are therefore used in this work.

RESULTS

Table 4 Experimental VLE Data of the liquid [$w_{2,liquid}$ (mass basis) and x_3] and vapor (y_1 and y_2) phases for the ternary system ethylene glycol (1) + water (2) + methane (3) at Temperature T and Pressure p. Standard uncertainties u are u(T) = 0.05 K and u(p) = $2 \cdot 10^{-3}$p. The expanded uncertainties for compositions (0.997 level of confidence) are reported in Table S1.

Exp. No.	T/K	p/MPa	10^2 $w_{2,\mathrm{liquid}}$	x_3	y_1/ppm	y_2/ppm
1	288.20	5.93	10.36	0.00478	1.2	91.1
2	293.13	6.00	10.37	0.00472	1.9	113
3	298.29	5.99	10.34	0.00484	3.1	148
4	303.14	6.00	10.19	0.00464	-	211
5	313.15	6.01	10.27	0.00487	-	315
6	323.16	5.99	10.24	0.00481	-	553
7	288.16	12.53	10.60	0.00818	1.9	57.1
8	293.14	12.47	10.37	0.00832	2.8	71.5
9	298.29	12.47	10.12	0.00847	4.0	94.8
10	303.14	12.50	10.17	0.00851	-	123
11	313.15	12.49	10.29	0.00880	-	188
12	323.19	12.50	10.26	0.00856	-	342
13	298.23	5.99	5.01	0.00631	3.7	94.2
14	298.23	12.47	4.98	0.01075	4.3	58.7
15	298.18	5.98	1.13	0.00708	4.5	30.8
16	298.17	12.47	1.09	0.01247	5.9	19.5

A total of sixteen experiments are reported in Table 4 and compositional uncertainties are provided in Table S1 (see Supporting Information). Three different experimental data types (y_1, y_2 and x_3) are evaluated graphically according to three factors (*T, p* and *glycol/water content*). Model performance for CPA is measured against experimental data according to average absolute relative deviation (AARD) expressed as a percentage:

$$AARD = \frac{1}{n}\sum_{i=1}^{n}\left|\frac{i_{model} - i_{exp}}{i_{exp}}\right| \cdot 100 \quad [\%]$$

Eq. 8

Details with regards to the model error calculations can be found in Tables S2-S7 (see Supporting Information).

RESULTS: Water in gas

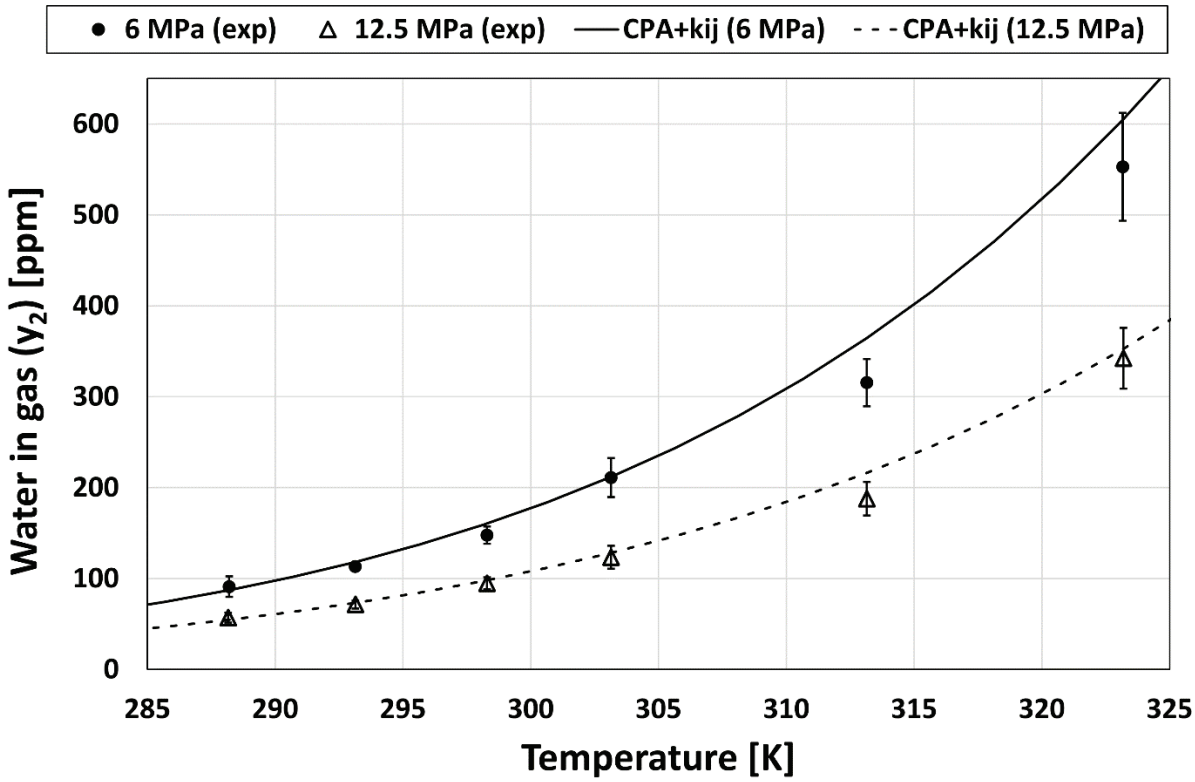

Figure 2 Results of the KF water content analysis for the vapor phase (y_2) of ethylene glycol (1) + water (2) + methane (3) at T = (288 – 323) K and with a constant MEG feed content of 90 wt%.

Figure 2 evaluates the effect of both temperature and pressure on the water content in the vapor phase. At the lower pressure of 6.0 MPa, vapor water content increases roughly exponentially with temperature from 100 to 550 ppm. At 12.5 MPa, a ~40% decrease the water content of the vapor phase is observed with values ranging from 60 to 350 ppm. The average relative standard deviation for the measurements (both data sets) is 2.8 %, giving an experimental uncertainty (± 3σ) of ± 8.6 %. The CPA model provides a good description of the data (AARD = 6 %), but generally over predicts the experimental data for T > 303 K. The prediction is, however, at or near the upper limit

of the experimental error. The experimental data and models in Figure 2 highlight the effect of the temperature and pressure as thermodynamic mechanisms for natural gas dehydration:

- higher pressure forces larger quantities of water into the liquid
- lower temperatures allow for more water to condense into the liquid

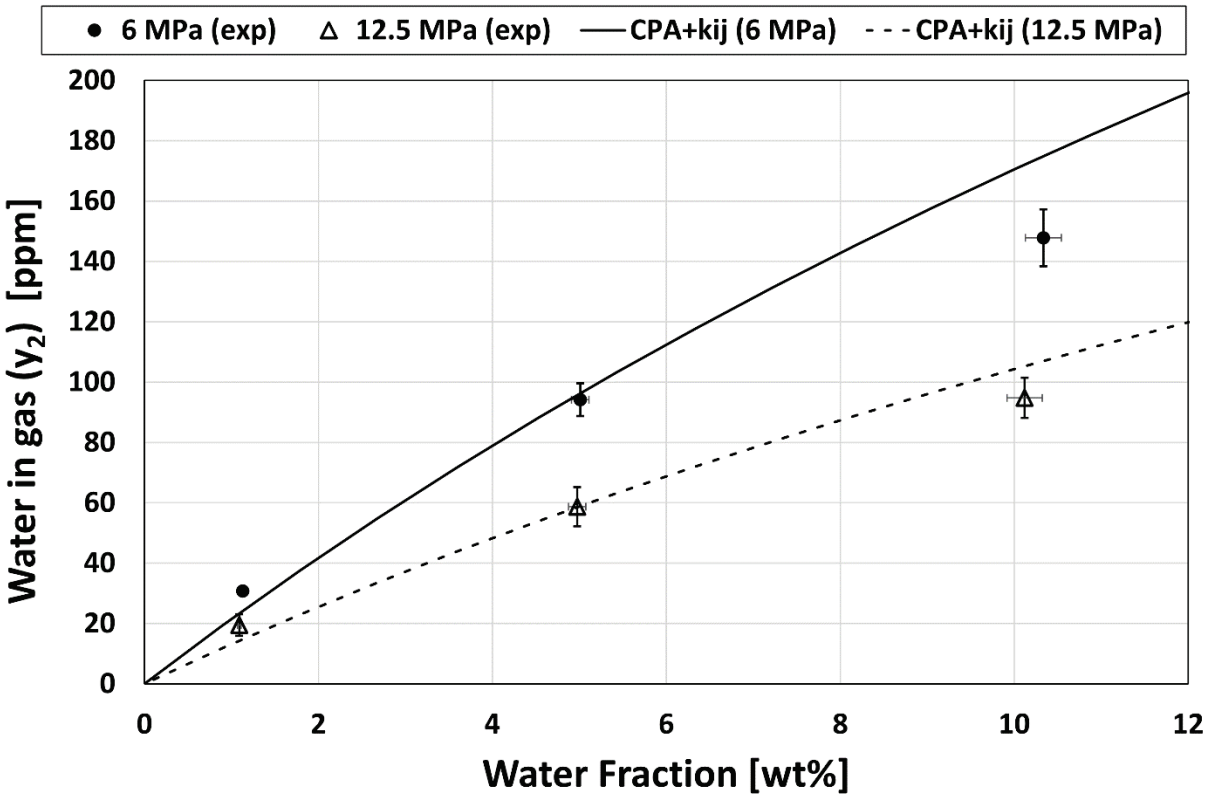

Figure 3 Results of the KF water content analysis for the vapor phase (y_2) of ethylene glycol (1) + water (2) + methane (3) with MEG feed content = (90 – 99) wt% at T = 298 K.

The vapor phase water content is evaluated according to the water content in the liquid phase in Figure 3. The water content in the vapor phase naturally increases as the liquid phase water content increases. Values of between 20 and 150 ppm are observed, while the relative standard deviations for the respective isobars indicate an experimental uncertainty of ± 5 %.

The CPA model qualitatively describes the experimental data, with the overall AARD of 13 %. While the data are over predicted at the higher water fractions, under prediction occurs at the lowest water fraction (1 %) where the measurements are more challenging. For this reason, several parallel measurements were taken.

Given the data measured here, a relatively pure glycol would be required to meet the water content (in gas) specification for operation at 298 K. Combining these results with mechanisms discussed for Figure 2, it can be seen that a low temperature, high pressure and high purity glycol would be ideal for natural gas dehydration.

RESULTS: MEG in gas

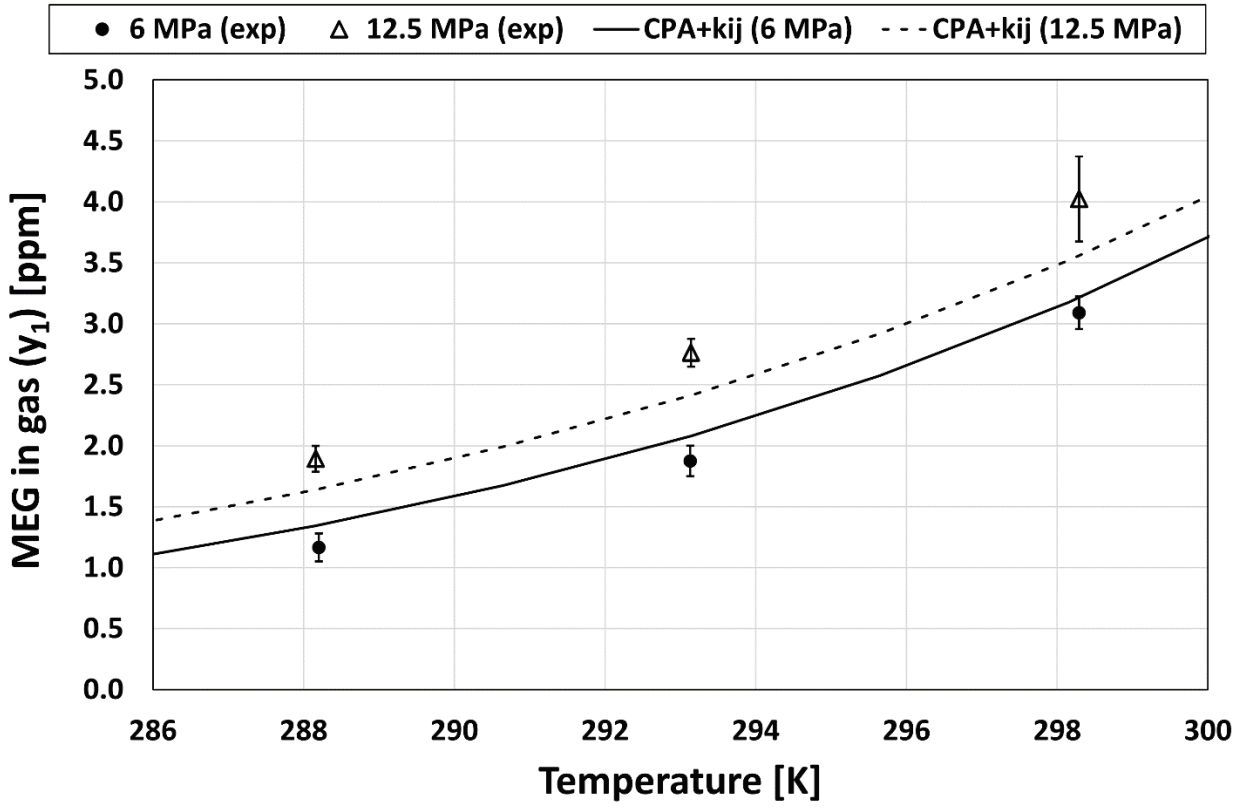

Figure 4 Results of the GC-MS MEG content analysis for the vapor phase (y_1) of ethylene glycol (1) + water (2) + methane (3) at T = (288 – 298) K and with a constant MEG feed content of 90 wt%.

Figure 4 presents the data from the GC-MS analyses of the MEG adsorbed onto ATD tubes. In general, it is seen that higher pressure results in slightly higher MEG content in the vapor phase while an increase in temperature leads to an exponential increase of y_1. The parallel measurements exhibit an average relative standard deviation of 3.8 %, yielding an experimental uncertainty of ± 11.5 %. We believe the high temperature measurements to be in error, due to insufficient flushing and glycol adsorption onto the metal tubing of the sampling pathway. The GC-MS method is likely

also unsuitable for the higher quantities of glycol in these experiments. For this reason, the experimental results are not published in Table 4.

The CPA model again provides a satisfactory qualitative prediction of the experimental data for lower temperatures (T < 300 K), although the high pressure data is under predicted (AARD = 12.7 %) while the low pressure data is over predicted (AARD = 9.8 %).

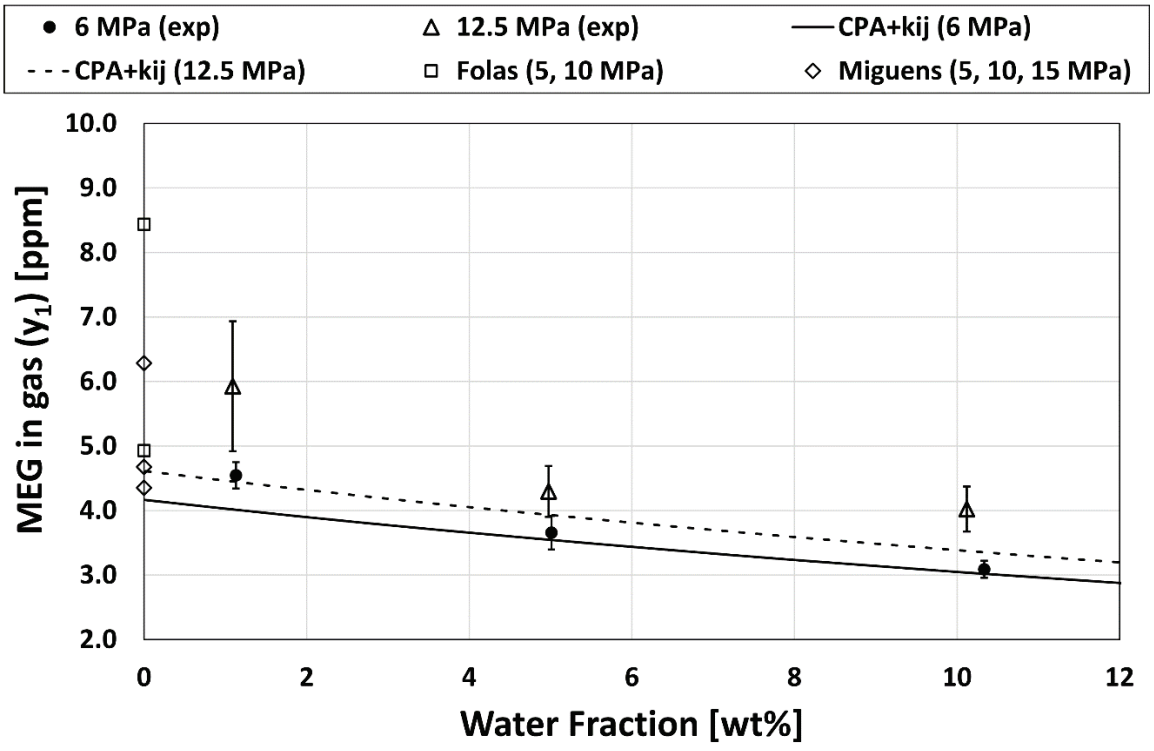

Figure 5 Results of the GC-MS MEG content analysis for the vapor phase (y_1) of ethylene glycol (1) + water (2) + methane (3) with MEG feed content = (90 – 99) wt% at T = 298 K.

Figure 5 presents the MEG vapor phase composition with varying MEG feed content. A mild exponential decrease is seen for the newly measured experimental data, from 6 to 4 and 4.5 to 3 ppm MEG at 12.5 and 6.0 MPa respectively. The experimental uncertainty is determined as ± 8.5 %. If the data is extrapolated towards the binary data available in the literature[8,12], a relatively fair

comparison is achieved. It is noted that our data aligns better with Miguens *et al*. at high pressure and Folas *et al*. at low pressure. Although a direct comparison is not possible, the differences appear to be within the experimental uncertainties quoted in the various sources.

The CPA model under predicts the experimental data (including the binary data of Folas *et al.* and Miguens *et al*.), although the error is greater for the data at 12.5 MPa (AARD = 18.1 %) as compared to 6.0 MPa (AARD = 5.7 %). It is again noticeable that CPA does not describe the low water content data well. It is also noted that from the standpoint of minimizing glycol carry-over to the vapor phase, a low pressure and higher water content are preferable. Therefore the design of a natural gas dehydration unit at high pressure would necessarily have to consider the trade-off between the water and glycol specifications in terms of finding the optimal operating pressure and glycol purity. In both cases, lowering the temperature is a mechanism for improved dehydration.

RESULTS: Dissolved CH_4

Whereas the experimental data presented in Figures 2-5 are directly measured, the dissolved methane content (x_3) is calculated using several measured variables. The temperature dependent dissolved methane content is presented in Figure 6.

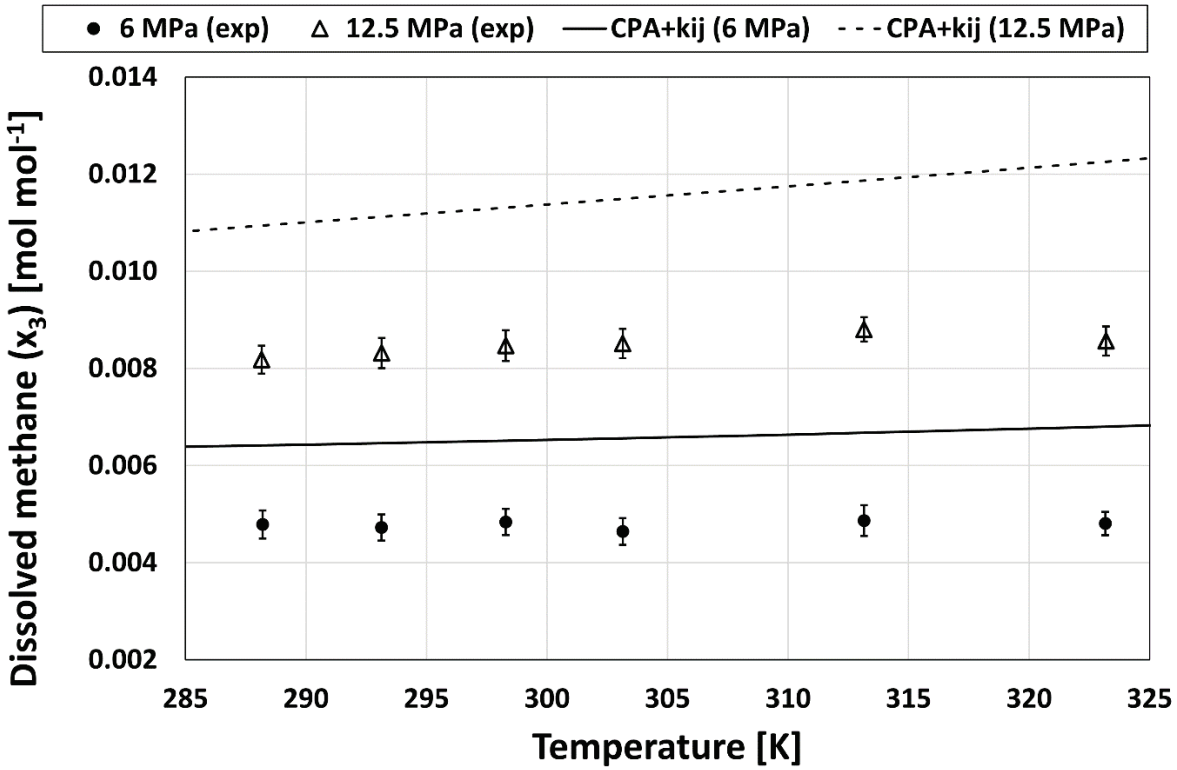

Figure 6 Dissolved methane content calculation for the liquid phase (x_3) of ethylene glycol (1) + water (2) + methane (3) at T = (288 – 323) K and with a constant MEG feed content of 90 wt%.

The calculated data reveals only a very slight temperature dependency, with dissolved methane content of approximately 0.005 and 0.008 mol·mol^{-1} at 6.0 and 12.5 MPa respectively. The relative standard deviations yield an uncertainty of less than ± 2 %.

CPA over predicts the dissolved methane content by 37 %, while Folas *et al.*[8] found an under prediction of almost 25 % using the same CPA parameters. There is however a significant disparity in the MEG-H_2O feed ratios between the two studies. Previously it has been shown that CPA cannot accurately account for both phases of the MEG + CH_4 binary system[3,14], although Boesen

et al.[14] were able to model both phases accurately using the SRK model with the Huron & Vidal[16] mixing rules.

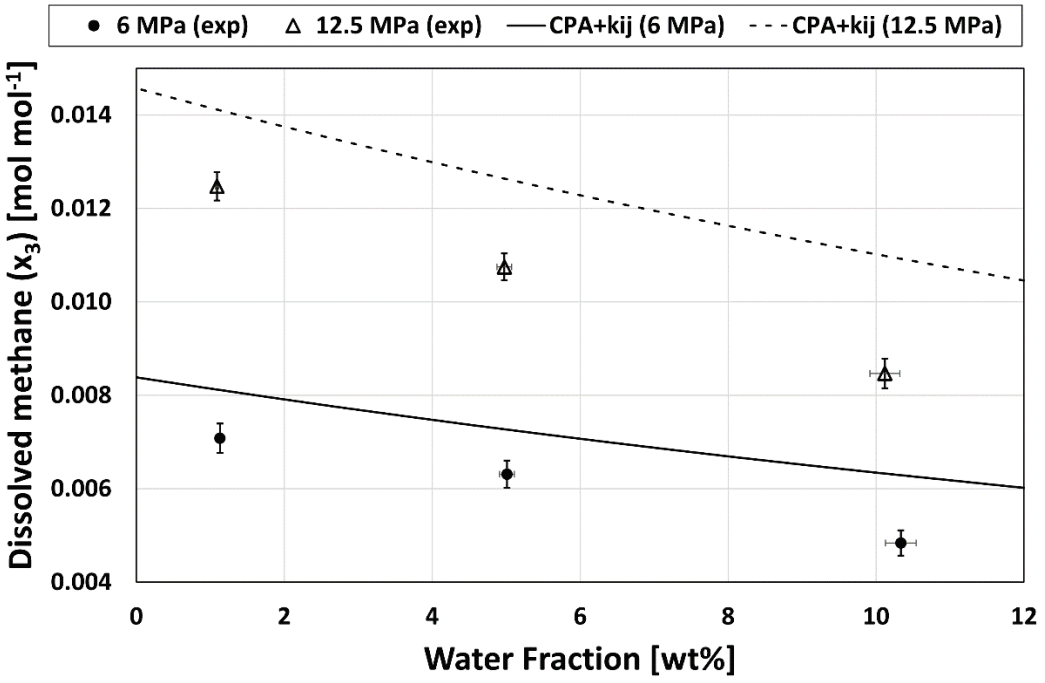

Figure 7 Dissolved methane content calculation for the liquid phase (x_3) of ethylene glycol (1) + water (2) + methane (3) with MEG feed content = (90 – 99) wt% at T = 298 K.

Figure 7 shows that dissolved methane increases with increasing pressure and decreases with increasing water content. This indicates that methane preferentially dissolves in MEG. The 12.5 MPa isobaric data decreases from 0.012 to 0.008 while the 6.0 MPa data decreases from 0.007 to 0.005. A ratio of approximately 1.7 is observed between the isobars. The experimental uncertainty is in line with that for the temperature dependent data.

As was previously the case for dissolved methane predictions, CPA over predicts the experimental data. The AARD is calculated as 20.9 %. Although there are only three data points for each isobar, it is noted that the magnitude of the error increases proportionally with water content.

Although the CPA model is over-estimating the interaction between methane and the liquid components, this may be considered as safety factor in terms of the design for the glycol regeneration unit.

The modeling results and experimental uncertainties are summarized in Table 5. It is seen that the overall modeling and experimental error are comparable for the associating compounds in the vapor phase while the modeling errors are significantly larger than the experimental errors for the fraction of gas dissolved into the liquid phase.

Table 5 Summary of experimental results and modeling errors

		Experimental Grouping				
		A	B	C	D	ALL
MEG Feed / wt%		90	90	90-99	90-99	
T / K		288-323	288-323	298	298	
p / MPa		6.0	12.5	6.00	12.5	
y_2	*u(exp)* / %	8.3	8.8	4.4	5.6	8.7
	$AARD_{CPA}$ / %	7.0	5.2	14	13	8.5
y_1	*u(exp)* / %	12	11	5.3	12	11
	$AARD_{CPA}$ / %	9.6	13	5.7	18	12
x_3	*u(exp)* / %	1.9	1.2	1.6	0.98	1.5
	$AARD_{CPA}$ / %	38	36	20	20	31

CONCLUSIONS

Phase equilibrium data is essential for the design of novel subsea natural gas dehydration installations. For this purpose, sixteen new data points have been measured for the ternary system: ethylene glycol (1) + water (2) + methane (3). Three independent variables were considered in this study:

- T = (288.15 – 323.15) K
- p = (6.0, 12.5) MPa
- overall MEG content = (90, 95, 99) wt%

KF Coulometry is used to measure the vapor phase water content (y_2), with values as high as 550 ppm and an experimental uncertainty (± 3σ) determined as ± 8.7 %. At a constant MEG/H_2O feed ratio, y_2 increases exponentially with temperature while an approximate doubling of the pressure leads to a 40 % decrease in y_2. CPA yields a good qualitative description of the data, with an over prediction (~ 10 %) which appears to decrease as water content in the mixture decreases.

The determination of MEG vapor phase composition (y_1) is achieved through adsorption and subsequent thermal desorption into a GC-MS. The highest MEG vapor content was determined as 12 ppm and the experimental uncertainty was calculated at ± 11.5 %. CPA yields good predictions at lower temperatures (T < 303 K) where the modeling error is approximately 12 %. For lower water fractions, the model is unable to accurately predict the increasing MEG content in the vapor phase.

Methane solubility (x_3) is calculated using, amongst other measured quantities, the volume of gas liberated from the liquid sample. The data shows only a very slight temperature dependency for the measured range, with values of approximately 0.005 and 0.008 at 6.0 and 12.5 MPa

respectively. Methane solubility is shown to decrease as water content increases. While the CPA model over predicts the experimental data quite significantly (>20 % AARD), the model does capture the general behavior of the data.

For both y_1 and y_2, the modeling error has approximately the same magnitude as the experimental error, but for x_3 the modeling error is an order of magnitude greater than the experimental error. From a process design perspective, the predictions of CPA can be used for feasibility studies related to the product quality of natural gas dehydration units, but the over prediction of x_3 should be taken into account for the design of glycol regeneration units and predictions of the volume of sales gas. The newly measured data supports the application of subsea natural gas dehydration at high pressure, with lower temperatures also being advantageous. The data however indicates that high MEG fractions will be required to sufficiently dehydrate the gas, but this in turn leads to increased MEG vapor content.

NOMENCLATURE

List of Symbols

Symbol	Description	Units
b	Co-volume	$cm^3 \cdot mol^{-1}$
c_1	attractive energy temperature-correction	-
g	Radial distribution function	-
M	molar mass	$g \cdot mol^{-1}$
m	mass	g
n	number of moles	mol
p	Pressure	MPa
R	Universal gas constant = 8.314	$J \cdot mol^{-1} \cdot K^{-1}$
T	Temperature	K
V	Volume	ml
V_m	Molar volume	$L \cdot mol^{-1}$
w_i	Mass fraction of component i	$g \cdot g^{-1}$
x_i	Liquid molar fraction of component i	$mol \cdot mol^{-1}$
y_i	Vapor molar fraction of component I	$mol \cdot mol^{-1}$

z_i	Molar feed fraction of component i	$mol \cdot mol^{-1}$
β	Volume of association	-
ε/R	Reduced association energy	K
Γ	Reduced attractive energy parameter = $a_0/(b_0 \cdot R)$	K
σ	Standard deviation	
ρ	Density	$g \cdot cm^{-3}$
ρ_m	Molar density	$mol \cdot L^{-1}$

Abbreviations

AARD	Average absolute relative deviation (see Eq. 8)
AI	Analyzer Indicator
ARD	Absolute relative deviation
assoc	Association - with respect to intermolecular forces
ATD	Auto Thermal Desorption
CPA	Cubic-Plus-Association equation of state (see equations 1-7)
FI	Flow Indicator
GC-MS	Gas Chromatography – Mass Spectrometry

HV	Huron-Vidal mixing rule
KF	Karl Fischer
MEG	Mono-ethylene glycol / ethylene glycol / 1,2-ethanediol
PC	Pressure Controller
PI	Pressure Indicator
PT	Pressure Transmitter
sPC-SAFT	Simplified Perturbed Chain SAFT equation of state
SAFT	Statistical Associating Fluid Theory equation of state
SRK	Soave-Redlich-Kwong equation of state
TA	Thermal Adsorption
TC	Temperature Controller
TI	Temperature Indicator
TT	Temperature Transmitter

ASSOCIATED CONTENT

Supporting Information

The supporting information includes the experimental data uncertainty, x_3 and y_1 calculation methods, and CPA model error calculations for each experimental data point.

AUTHOR INFORMATION

Corresponding Author

Nicolas von Solms

E-mail: nvs@kt.dtu.dk

Author Contributions

The manuscript was written through contributions of all authors. All authors have given approval to the final version of the manuscript.

Acknowledgment

The authors gratefully acknowledge the financial support from Statoil A/S (Norway) for this work as part of the research project 'Thermodynamics of Petroleum Fluids relevant to Subsea Processing' which is part of the 'Chemicals in Gas Processing' joint industry project. The authors thank Statoil A/S (Norway) for permission to publish the data.

REFERENCES

(1) Fredheim, A. O.; Johnsen, C. G.; Johannessen, E.; Kojen, G. P. Gas-2-Pipe^{TM}, A Concept for Treating Gas to Rich Gas Quality in a Subsea or Unmanned Facility. *Annu. Offshore Technol. Conf., Proc.*, Houston, **2016**.

(2) GASSCO. Terms and conditions for transportation of gas in the GASSLED http://www.gassco.no/contentassets/40e7d932034346caaa7ac647bcd9ee6f/terms-and-conditions-01.07.2017---incl.-appendix.pdf (accessed Aug 22, 2017). **2017**.

(3) Kruger, F.; Kontogeorgis, G. M.; von Solms, N. New Association Schemes for Mono-Ethylene Glycol: Cubic-Plus-Association Parameterization and Uncertainty Analysis. *Fluid Phase Equilib.* **2018**, 458, 211–233.

(4) Jou, F. Y.; Otto, F. D.; Mather, A. E. Solubility of Methane in Glycols at Elevated Pressures. *Can. J. Chem. Eng.* **1994**, 72, 130–133.

(5) Zheng, D.-Q.; Ma, W.-D.; Wei, R.; Guo, T.-M. Solubility Study of Methane, Carbon Dioxide and Nitrogen in Ethylene Glycol at Elevated Temperatures and Pressures. *Fluid Phase Equilib*. **1999**, 155, 277–286.

(6) Wang, L.-K.; Chen, G.-J.; Han, G.-H.; Guo, X.-Q.; Guo, T.-M. Experimental Study on the Solubility of Natural Gas Components in Water with or without Hydrate Inhibitor. *Fluid Phase Equilib.* **2003**, 207, 143–154.

(7) Jou, F.-Y.; Schmidt, K. A. G.; Mather, A. E. Vapor–liquid Equilibrium in the System Ethane+ethylene Glycol. *Fluid Phase Equilib.* **2006**, 240, 220–223.

(8) Folas, G. K.; Berg, O. J.; Solbraa, E.; Fredheim, A. O.; Kontogeorgis, G. M.; Michelsen, M. L.; Stenby, E. H. High-Pressure Vapor–liquid Equilibria of Systems Containing Ethylene Glycol, Water and Methane: Experimental Measurements and Modeling. *Fluid Phase Equilib*. **2007**, 251, 52–58.

(9) Abdi, M. A.; Hussain, A.; Hawboldt, K.; Beronich, E. Experimental Study of Solubility of Natural Gas Components in Aqueous Solutions of Ethylene Glycol at Low-Temperature and High-Pressure Conditions. *J. Chem. Eng. Data* **2007**, 52, 1741–1746.

(10) Galvão, A. C.; Francesconi, A. Z. Solubility of Methane and Carbon Dioxide in Ethylene Glycol at Pressures up to 14 MPa and Temperatures Ranging from (303 to 423) K. *J. Chem. Thermodyn*. **2010**, 42, 684–688.

(11) Frost, M. Measurement and Modelling of Phase Equilibrium of Oil - Water - Polar Chemicals. PhD, Technical University of Denmark: Kgs. Lyngby, **2014**.

(12) Miguens, A. C. M.; Solbraa, E.; Hansen, A. B.; Løkken, T. V.; Haugum, T.; Solvang, S. Glycols in Natural Gas - Experiments, Modelling and Tracking. *International Gas Union Research Conference, Copenhagen*, **2014**.

(13) Ng, H.-J.; Chen, C.-J. Vapour−Liquid and Vapour−Liquid−Liquid Equilibria for H2S, CO2, Selected Light Hydrocarbons and a Gas Condensate in Aqueous Methanol or Ethylene Glycol Solutions. *Gas Processors' Association (GPA)* **1995**.

(14) Boesen, R. R.; Herslund, P. J.; Sørensen, H. Loss of Monoethylene Glycol to CO_2- and H_2S-Rich Fluids: Modeled Using Soave–Redlich–Kwong with the Huron and Vidal

Mixing Rule and Cubic-Plus-Association Equations of State. *Energy Fuels* **2017**, 31, 3417–3426.

(15) Soave, G. Equilibrium Constants from a Modified Redlich-Kwong Equation of State. *Chem. Eng. Sci.* **1972**, 27, 1197–1203.

(16) Huron, M.-J.; Vidal, J. New Mixing Rules in Simple Equations of State for Representing Vapour-Liquid Equilibria of Strongly Non-Ideal Mixtures. *Fluid Phase Equilib.* **1979**, 3, 255–271.

(17) Kristensen, J. N.; Christensen, P. L.; Pedersen, K. S.; Skovborg, P. A Combined Soave-Redlich-Kwong and NRTL Equation for Calculating the Distribution of Methanol between Water and Hydrocarbon Phases. *Fluid Phase Equilib*. **1993**, 82, 199–206.

(18) Kontogeorgis, G. M.; Voutsas, E. C.; Yakoumis, I. V.; Tassios, D. P. An Equation of State for Associating Fluids. *Ind. Eng. Chem. Res.* **1996**, 35, 4310–4318.

(19) Kontogeorgis, G. M.; V. Yakoumis, I.; Meijer, H.; Hendriks, E.; Moorwood, T. Multicomponent Phase Equilibrium Calculations for Water–methanol–alkane Mixtures. *Fluid Phase Equilib*. **1999**, 158–160, 201–209.

(20) Liang, X.; Aloupis, G.; Kontogeorgis, G. M. Data Requirements and Modeling for Gas Hydrate-Related Mixtures and a Comparison of Two Association Models. *J. Chem. Eng. Data* **2017**, 62, 2592-2605.

(21) Haghighi, H.; Chapoy, A.; Burgess, R.; Tohidi, B. Experimental and Thermodynamic Modelling of Systems Containing Water and Ethylene Glycol: Application to Flow Assurance and Gas Processing. *Fluid Phase Equilib*. **2009**, 276, 24–30.

(22) Mazloum, S.; Chapoy, A.; Yang, J.; Tohidi, B. A Novel Technique for Monitoring Hydrate Safety Margin; *SPE Prod. Oper*. **2011**, 27, 376-381.

(23) Tzirakis, F.; Karakatsani, E.; Kontogeorgis, G. M. Evaluation of the Cubic-Plus-Association Equation of State for Ternary, Quaternary, and Multicomponent Systems in the Presence of Monoethylene Glycol. *Ind. Eng. Chem. Res.* **2016**, 55, 11371–11382.

(24) dos Santos, L. C.; Abunahman, S. S.; Tavares, F. W.; Ruiz Ahón, V. R.; Kontogeorgis, G. M. Cubic Plus Association Equation of State for Flow Assurance Projects. *Ind. Eng. Chem. Res.* **2015**, 54, 6812–6824.

(25) Yarveicy, H.; Ghiasi, M. M. Modeling of Gas Hydrate Phase Equilibria: Extremely Randomized Trees and LSSVM Approaches. *J. Mol. Liq*. **2017**, 243, 533–541.

(26) Yarveicy, H.; Ghiasi, M. M.; Mohammadi, A. H. Determination of the Gas Hydrate Formation Limits to Isenthalpic Joule–Thomson Expansions. *Chem. Eng. Res. Des*. **2018**, 132, 208–214.

(27) Kontogeorgis, G. M.; Folas, G. K. Chapter 9: The Cubic-Plus-Association Equation of State. In *Thermodynamic Models for Industrial Applications*. John Wiley & Sons, Ltd. **2010**, pp 261–297.

(28) Derawi, S. O.; Michelsen, M. L.; Kontogeorgis, G. M.; Stenby, E. H. Application of the CPA Equation of State to Glycol/Hydrocarbons Liquid–liquid Equilibria. *Fluid Phase Equilib*. **2003**, 209, 163–184.

(29) Tsivintzelis, I.; Kontogeorgis, G. M.; Michelsen, M. L.; Stenby, E. H. Modeling Phase Equilibria for Acid Gas Mixtures Using the CPA Equation of State. I. Mixtures with H_2S. *AIChE J.* **2010**, 56, 2965–2982.

(30) Kontogeorgis, G. M.; Tsivintzelis, I.; von Solms, N.; Grenner, A.; Bøgh, D.; Frost, M.; Knage-Rasmussen, A.; Economou, I. G. Use of Monomer Fraction Data in the Parametrization of Association Theories. *Fluid Phase Equilib*. **2010**, 296, 219–229.

(31) Kontogeorgis, G. M.; Folas, G. K.; Muro-Suñé, N.; von, S.; Michelsen, M. L.; Stenby, E. H. Modelling of Associating Mixtures for Applications in the Oil & Gas and Chemical Industries. *Fluid Phase Equilib*. **2007**, 261, 205–211.

Supporting Information

Ternary vapor-liquid equilibrium measurements and modeling of ethylene glycol (1) + water (2) + methane (3) systems at 6 and 12.5 MPa

Francois J. Kruger[‡], *Marie V. Danielsen*[†], *Georgios M. Kontogeorgis*[‡], *Even Solbraa*[†], *Nicolas von Solms*[‡,*]

‡ Department of Chemical and Biochemical Engineering, Center for Energy Resources Engineering (CERE), Technical University of Denmark, DK-2800, Lyngby, Denmark

† Statoil ASA, Research and Development Center, N-7005, Trondheim, Norway

* Corresponding author e-mail: nvs@kt.dtu.dk

DATA UNCERTAINTY

Table S1 Uncertainty (3σ) for experimental VLE Data of the liquid [$w_{2,liquid}$ (mass basis) and x_3] and vapor (y_1 and y_2) phases for the ternary system ethylene glycol (1) + water (2) + methane (3)

Exp. No.	$10^2\ w_{2,liquid}$	$x_3\ 10^4$	y_1/ppm	y_2/ppm
1	0.064	2.90	0.11	11.3
2	0.085	2.69	0.13	2.2
3	0.106	2.70	0.13	9.4
4	0.042	2.74	-	21.4
5	0.042	3.18	-	26.0
6	0.021	2.41	-	59.4
7	0.125	2.89	0.11	5.5
8	0.042	3.11	0.11	4.6
9	0.042	3.17	0.35	6.6
10	0.064	3.03	-	12.6
11	0.064	2.52	-	18.5
12	0.021	3.00	-	33.4
13	0.085	2.92	0.26	5.4
14	0.064	2.89	0.40	6.5
15	0.000	3.14	0.20	0.3
16	0.000	3.04	1.01	3.6

CALCULATIONS FOR EXPERIMENTAL VALUES

Calculation of dissolved methane fraction

$$n_{H2O} = \frac{w_{2,liquid}}{100 \cdot M_{H2O}} \times m_{liq\ sample}$$

Eq. S1

$$n_{MEG} = \frac{\left(100 - w_{2,liquid}\right)}{100 \cdot M_{MEG}} \times m_{liq\ sample}$$

Eq. S2

$$n_{CH4} = \frac{pV}{RT} = \frac{p_{GM} \cdot \left(\Delta V_{GM} - \frac{m_{liq\ sample}}{\rho_{liq\ sample}}\right)}{R \cdot T_{GM}}$$

Eq. S3

$$x_{CH4} = \frac{n_{CH4}}{n_{MEG} + n_{H2O} + n_{CH4}}$$

Eq. S4

The following experimentally determined values are used in the above calculations:

- w_2 [%wt$_{H2O}$] is the result from KF analysis of the liquid sample
- $m_{liq\ sample}$ and $\rho_{liq\ sample}$ are the mass and density measurements done on the liquid sample
- p_{GM}, ΔV_{GM} and T_{GM} are the pressure, change in volume and temperature of recorded in the gas meter

Calculation of MEG vapor fraction

$$n_{MEG} = \frac{m_{MEG\ (GC-MS)}}{M_{MEG}}$$

Eq. S5

$$n_{gas} = \frac{pV}{RT} = \frac{p_{atm} \cdot (\Delta V_{GasClock})}{R \cdot T_{atm}}$$

Eq. S6

$$y_{MEG} = \frac{n_{MEG}}{n_{MEG} + n_{gas}}$$

Eq. S7

For the calculations in equations S5-S7, $m_{MEG\ (GC\text{-}MS)}$ is the result of GC-MS analysis. The atmospheric pressure and temperature were measured using gauges fitted to the gas clock and would vary between 96 – 98 kPa and 295 – 296 K within the controlled laboratory setting. The sensitivity of y_{MEG} to these variations was shown as a minor effect on the 2nd and 3rd significant figure for pressure and temperature respectively.

ERROR CALCULATIONS FOR THERMODYNAMIC MODELS

Table S2 Water in gas (y_2) error calculations for CPA at T = 298 K in Figure 3

p / MPa	$10^2\ w_2$ (exp) / wt%	y_2 (CPA) / ppm	*ARD* / %	*AARD* / %
6.0	1.13	24.1	21.7	
6.0	5.01	96.2	2.2	14.0
6.0	10.34	174.8	18.3	
12.5	1.09	14.2	27.1	
12.5	4.98	58.4	0.6	12.8
12.5	10.12	105.0	10.8	
		Overall AARD		13.4

Table S3 Glycol in gas (y_1) error calculations for CPA at T = 298 K in Figure 5

p / MPa	$10^2\ w_2$ (exp) / wt%	y_1 (CPA) / ppm	*ARD* / %	*AARD* / %
6.0	1.13	4.0	11.8	
6.0	5.01	3.5	3.1	5.7
6.0	10.34	3.0	2.3	
12.5	1.09	4.5	24.9	
12.5	4.98	3.9	13.5	18.1
12.5	10.12	3.4	16.1	
		Overall AARD		11.9

Table S4 Dissolved CH_4 (x_3) error calculations for CPA at T = 298 K in Figure 7

p / MPa	$10^2\ w_2$ (exp) / wt%	$x_3\ 10^4$ (CPA) / ppm	*ARD* / %	*AARD* / %
6.0	1.13	81.1	14.6	
6.0	5.01	72.7	15.2	19.9
6.0	10.34	62.9	30.0	
12.5	1.09	141.2	13.2	
12.5	4.98	126.4	17.6	20.2
12.5	10.12	110.0	29.8	
		Overall AARD		20.1

Table S5 Water in gas (y_2) error calculations for CPA for a constant MEG feed of 90 wt% in Figure 2

T / K	p / MPa	y_2 (CPA) / ppm	*ARD* / %	*AARD* / %
288	6.0	86.9	4.6	7.0
293	6.0	118.3	4.4	
298	6.0	159.2	7.7	
303	6.0	211.9	0.4	
313	6.0	364.5	15.5	
323	6.0	603.9	9.2	
288	12.5	54.5	4.4	5.2
293	12.5	73.3	2.4	
298	12.5	97.4	2.7	
303	12.5	128.2	3.9	
313	12.5	216.1	15.1	
323	12.5	352.0	2.8	
		Overall AARD		6.1

Table S6 Glycol in gas (y_1) error calculations for CPA for a constant MEG feed of 90 wt% in Figure 4

T / K	p / MPa	y_1 (CPA) / ppm	*ARD* / %	*AARD* / %
288	6.0	1.34	15.2	9.6
293	6.0	2.08	10.9	
298	6.0	3.17	2.73	
303	6.0	4.77	-	
313	6.0	10.35	-	
323	6.0	21.33	-	
288	12.5	1.64	13.4	12.9
293	12.5	2.41	12.6	
298	12.5	3.52	12.6	
303	12.5	5.07	-	
313	12.5	10.21	-	
323	12.5	19.74	-	
		Overall AARD		11.2

Table S7 Dissolved CH_4 (x_3) error calculations for a constant MEG feed of 90 wt% in Figure 6

T / K	p / MPa	$x_3\ 10^4$ (CPA) / ppm	*ARD* / %	*AARD* / %
288	6.0	64.13	34.0	
293	6.0	64.58	36.7	
298	6.0	65.07	34.5	
303	6.0	65.59	41.3	37.5
313	6.0	66.73	37.1	
323	6.0	68.00	41.5	
288	12.5	109.4	33.7	
293	12.5	111.2	33.8	
298	12.5	113.1	33.5	
303	12.5	114.9	35.0	35.6
313	12.5	118.7	34.8	
323	12.5	122.5	43.1	
		Overall AARD		36.6